RAA 2017 Vol. **17** No. **9**, 89 (14pp) doi: 10.1088/1674–4527/17/9/89

http://www.raa-journal.org *http://iopscience.iop.org/raa*

***R**esearch in*
***A**stronomy and*
***A**strophysics*

Combination of terrestrial reference frames based on space geodetic techniques in SHAO: methodology and main issues

Bing He[1,2,3], Xiao-Ya Wang[1,2,3], Xiao-Gong Hu[1,3] and Qun-He Zhao[1,2,3]

[1] Shanghai Astronomical Observatory, Chinese Academy of Sciences, Shanghai 200030, China; *hebing@shao.ac.cn*
[2] School of Astronomy and Space Science, University of Chinese Academy of Sciences, Beijing 100049, China
[3] State Key Laboratory of Aerospace Dynamics, Xi'an 710043, China

Received 2017 February 23; accepted 2017 April 14

Abstract Based on years of input from the four geodetic techniques (SLR, GPS, VLBI and DORIS), the strategies of the combination were studied in SHAO to generate a new global terrestrial reference frame as the material realization of the ITRS defined in IERS Conventions. The main input includes the time series of weekly solutions (or fortnightly for SLR 1983–1993) of observational data for satellite techniques and session-wise normal equations for VLBI. The set of estimated unknowns includes 3-dimensional Cartesian coordinates at the reference epoch 2005.0 of the stations distributed globally and their rates as well as the time series of consistent Earth Orientation Parameters (EOPs) at the same epochs as the input. Besides the final solution, namely SOL-2, generated by using all the inputs before 2015.0 obtained from short-term observation processing, another reference solution, namely SOL-1, was also computed by using the input before 2009.0 based on the same combination of procedures for the purpose of comparison with ITRF2008 and DTRF2008 and for evaluating the effect of the latest six more years of data on the combined results. The estimated accuracy of the x-component and y-component of the SOL-1 TRF-origin was better than 0.1 mm at epoch 2005.0 and better than 0.3 mm yr^{-1} in time evolution, either compared with ITRF2008 or DTRF2008. However, the z-component of the translation parameters from SOL-1 to ITRF2008 and DTRF2008 were 3.4 mm and –1.0 mm, respectively. It seems that the z-component of the SOL-1 TRF-origin was much closer to the one in DTRF2008 than the one in ITRF2008. The translation parameters from SOL-2 to ITRF2014 were 2.2, -1.8 and 0.9 mm in the x-, y- and z-components respectively with rates smaller than 0.4 mm yr^{-1}. Similarly, the scale factor transformed from SOL-1 to DTRF2008 was much smaller than that to ITRF2008. The scale parameter from SOL-2 to ITRF2014 was –0.31 ppb with a rate lower than 0.01 ppb yr^{-1}. The external precision (WRMS) compared with IERS EOP 08 C04 of the combined EOP series was smaller than 0.06 mas for the polar motions, smaller than 0.01 ms for the UT1-UTC and smaller than 0.02 ms for the LODs. The precision of the EOPs in SOL-2 was slightly higher than that of SOL-1.

Key words: astrometry — reference systems — techniques: interferometers — methods: data analysis

1 INTRODUCTION

A global Terrestrial Reference Frame (TRF), consisting of a set of globally distributed stations with precisely determined positions and velocities, is fundamental to positioning and navigation on Earth's surface, determination of the orbits of Earth-observing satellites and monitoring the changes of the Earth systems such as deformation of the solid surface of Earth and variation in the global sea level (Heflin et al. 2013; Blewitt 2003).

Since the 1960s, various space geodetic techniques such as Satellite Laser Ranging (SLR), Global Navigation Satellite System (GNSS), Very Long Baseline Interferometry (VLBI) and Doppler Orbitography and Radio-positioning Integrated by Satellites (DORIS) have made great progress with many

advances in the precision, global distribution and determination of Earth's center (Jin et al. 2013). Observations with high spatial and temporal resolutions provided by these techniques have allowed them to become the major measurement methods instead of traditional astronomic or geodetic techniques for the estimation of the global TRF and Earth Orientation Parameters (EOPs) (Jin et al. 2011).

The International Terrestrial Reference Frame (ITRF), as a realization of the International Terrestrial Reference System (ITRS), was developed at the ITRS Center of the International Earth Rotation and Reference Systems Service (IERS). It consists of a series of updated and improved versions rather than one single ITRF (Altamimi et al. 2007; Altamimi et al. 2011; Blewitt et al. 2010). The most recent release is ITRF2014, which is based on a time series of weekly or daily reprocessed solutions of station positions using the four space geodetic techniques and daily EOPs. ITRF2014 is improved compared to the past versions by an enhanced modeling of annual and semiannual signals of station motions and postseismic deformations caused by major earthquakes (Altamimi et al. 2016). Another institute performing the combination of TRFs and EOPs is the Deutsches Geodätisches Forschungsinstitut and Technische Universität München (DGFI-TUM) (Seitz et al. 2012; Bloßfeld et al. 2015; Angermann et al. 2009). DTRF2014 is DGFI-TUM's new realization of the ITRS. Both ITRF2014 and DTRF2014 consist of positions and velocities of globally distributed stations that use space geodetic observation techniques VLBI, SLR, GNSS and DORIS as well as consistently estimated EOPs.

Besides these two realizations of secular TRF, other work has been done by researchers concerning combinations of TRFs. Wu et al. (2015) used a Kalman filter and smoother approach to realize an experimental TRF through the time series of geocentric coordinates by combining SLR/GNSS/VIBI/DORIS data at the Jet Propulsion Laboratory (JPL). Deutsches GeoForschungsZentrum Potsdam (GFZ) applied a rigorous combination of datum-free normal equation systems of SLR, GPS and VLBI using original observation data spanning from the 290th day to the 304th day of 2002 with station positions, the EOPs and troposphere parameters as the major unknowns. They were actually concerned with the a priori models used for generating technique-specific normal equation systems, the identical parameterization chosen for common parameters and the combination of troposphere parameters (Thaller et al. 2008). Bloßfeld et al. (2014) investigated a new approach based on the weekly combination of epoch normal equations of GPS/SLR/VLBI data to generate a time series of epoch reference frames and then studied the advantages and disadvantages in detail compared to the conventional secular approach.

The availability of one more ITRS realization can help to analyze possible reasons for limited accuracy when a multi-year global TRF is computed. Comparisons of different realizations provide great potential in terms of validation and quality assessment as well as improving the reliability of the ITRF (Seitz et al. 2012; Seitz et al. 2013).

In this study, we used our strategies of combination to accomplish a new realization of the ITRS, differently and independently from the realizations in IGN or DGFI-TUM. Based on the combination procedure developed by Shanghai Astronomical Observatory (SHAO), two solutions, namely solution-1 (SOL-1) and solution-2 (SOL-2), have been computed by using different time spans of input data as the only difference. Each of these two solutions mainly includes positions and linear velocities of global stations and consistently combined daily EOPs. To validate the combination strategy and to crosscheck with ITRF2008 or DTRF2008, SOL-1 has the same input data source and time span as ITRF2008. SOL-2, as the final combined product, was obtained from the same type of input data as SOL-1 but with a time span extending to 2015.0 and was then compared with ITRF2014 for external calibration.

2 INPUTS

The combination strategy used in this thesis is based on four techniques: GPS, VLBI, SLR and DORIS. The input data are technique-specific estimations of global station coordinates and the EOP, in the form of weekly intra-combined solutions for the case of satellite techniques (Pavlis et al. 2014; Ferland & Piraszewski 2009; Valette et al. 2010) and session-wise normal equations for VLBI (Böckmann et al. 2010). Time series of these short-term solutions were then used as 'pseudo-observations' for the combination to generate long-term coordinate solutions and consistent EOP series. The data sets were provided by the specific Combination Centers (CCs) of the International Association of Geodesy (IAG): the International GNSS Service (IGS) (Dow et al. 2009), the International VLBI service for Geodesy and Astronomy (IVS) (Schuh & Behrend 2012), the International Laser

Ranging Service (ILRS) (Pearlman et al. 2002) and the International DORIS Service (IDS) (Willis et al. 2010).

In order to assess the impact of the combination strategy on TRF and EOP, two different time spans of input data were applied separately by our combination procedure to yield two combination solutions, called SOL-1 and SOL-2, under the same models and the same definition of TRF datum. The time span of SOL-1's input ends with 2009.0, which is the same as ITRF2008 and leads to a clear comparison between our combination and ITRF2008. The inputs of SOL-2 end with 2015.0 for comparison with ITRF2014.

Table 1 summarizes some characteristics including the time span, resolution, solution type and constraint of the input. It is worth noting that the loose constraint used for SLR means that there is an a priori standard deviation on station coordinates of $\sim$1 m and the equivalent of at least 1 m for EOPs (Pavlis et al. 2014). For more details regarding the minimum constraints, the reader may refer to Sillard & Boucher (2001).

3 METHOD

Different space geodetic techniques are sensitive to common geodetic parameters, e.g. station coordinates and EOPs (Kutterer et al. 2015). This is fundamental to the multi-technique combination of TRFs and EOPs. The combination strategy developed here consists of three main steps: (1) for each technique, generate a normal equation system by stacking time series of weekly solutions or session-wise normal equations of the station coordinates and the daily EOP; (2) combine the four technique-wise normal equation systems together by local ties and use different types of constraints for the datum definition to generate a global and multi-technique normal equation system; and (3) resolve the large-scale equation systems and iterate step (2) by re-weighting the four technique-specific normal equation systems deduced in step (1). An overview of the data flow and software used for the combination approach is shown in Figure 1.

3.1 Combination Strategy

As a realization of an ideal TRS, the currently most-used TRF type is a kinematical TRF with precisely determined coordinates of physical points (such as tracking stations of geodetic techniques) in a three-dimensional (3-D) Cartesian coordinate system.

Figure 2 illustrates a network of stations distributed globally that uses the four techniques. We applied a linear model to describe motion of the stations in multiple years, which means in a given multi-year TRF r, the 3-D Cartesian coordinates $X(x, y, z)$ of the station i in any epoch t, $X_r^i(t)$, can be expressed by the coordinates $X_r^i(t_0)$ at the reference epoch t_0 and its velocities $\dot{X}$ using the following equation

$$X_r^i(t) = X_r^i(t_0) + (t - t_0)\dot{X}_r^i \,. \tag{1}$$

For inputs of SLR, GPS and DORIS, short-term solutions of globally distributed positions of stations and daily EOPs using weekly observation data (or fortnightly for SLR 1983.0–1993.0) cover more than 10 yr, or even more than 20 yr. In a different way, VLBI provides session-wise normal equations instead. We call these types of short-term solutions a weekly solution or weekly input throughout the rest of this article. Assuming that each weekly solution has an underlying TRF which differs from the finally combined one, the transformation between the short-term TRF and the long-term combined one can be described by a Euclidean similarity transformation model (Petit & Luzum 2010) involving three translation parameters, three rotation parameters and one scale factor, which is well known as the 7-parameter transformation model and is currently widely used in astrometry and geodesy. By applying the linear model of station motion into the 7-parameter model, we can define the relationship between weekly station positions $X_{\rm s}(t_i)$ and the combined solution of coordinates and velocities as well as the relationship between daily EOP $X_{\rm s}^{\rm eop}(t_j)$ given in weekly solutions and the combined daily EOP by

$$\begin{pmatrix} X_{\rm s}(t_i) \\ X_{\rm s}^{\rm eop}(t_j) \end{pmatrix} = \phi(t, X_{\rm c}^0) \begin{pmatrix} X_{\rm c}(t_0) \\ \dot{X}_{\rm c} \\ X_{\rm c}^{\rm eop}(t_j) \\ H_7^s(t_k) \end{pmatrix}, \tag{2}$$

where $X_{\rm s}(t_i)$ and $X_{\rm s}^{\rm eop}(t_j)$ are the station coordinates at epoch t_i and the EOP at epoch t_j from weekly or daily input solution s. $X_{\rm c}(t_0)$ and $\dot{X}_{\rm c}$ are the coordinates at the reference epoch t_0 and the linear velocities for stations under the combined multi-year reference frame c. $X_{\rm c}^{\rm eop}(t_j)$ is the combined EOP value (polar motion, LOD or UT1-UTC) at epoch t_j consistent with the combined frame c. $H_7^s(t_k)$ is the set of transformation parameters between frames s and c.

Based on the theory of least squares adjustment by the Gauss-Markov model (Koch 2013), one can obtain

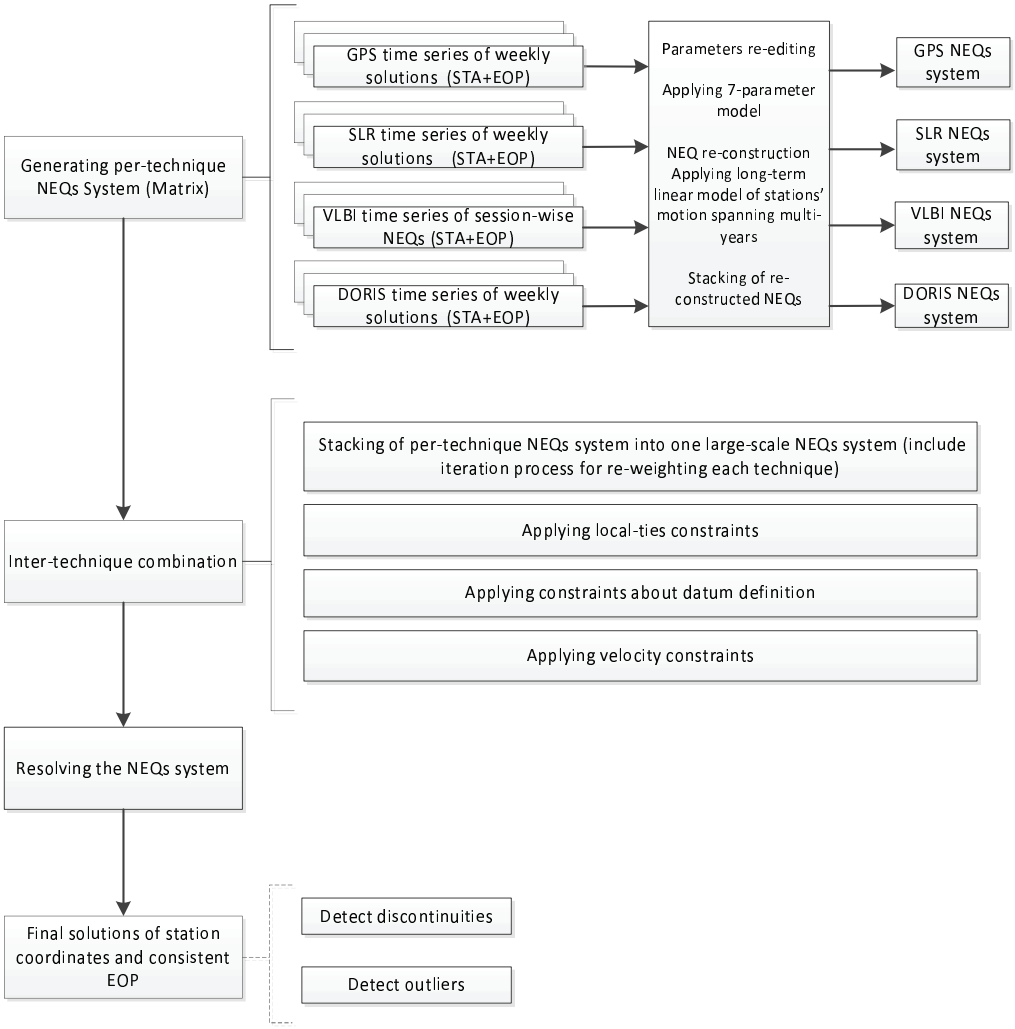

Fig. 1 A brief flowchart of the program used for the combination approach.

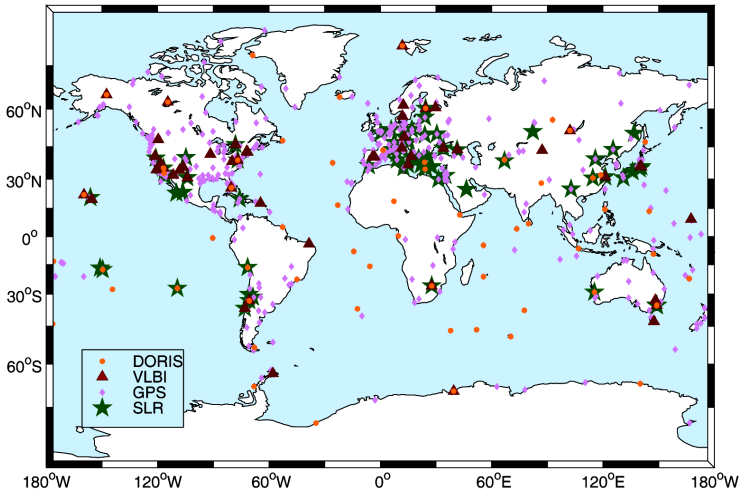

Fig. 2 Global distribution of GPS/SLR/VLBI/DORIS stations.

Table 1 Summary of Inputs for the Combination Solutions: SOL-1 and SOL-2

Technique	Combination Center	Analysis Center	Data Span	Solution Type	Constraints
SLR	ASI	ASI, DGFI, GFZ, JCET, etc.	SOL-1:1983.0–2009.0 SOL-2:1983.0–2015.0	Solution and Covariance matrix	Loose constraints
GPS	NRCan	CODE, ESOC, GFZ, JPL, etc.	SOL-1:1997.0–2009.0 SOL-2:1997.0–2015.0	Solution and Covariance matrix	Minimum constraints
VLBI	GIUB	BKG, DGFI, GSFC, SHAO, etc.	SOL-1:1980.0–2009.0 SOL-2:1980.0–2015.0	Normal Equation	Constraints free
DORIS	IGN	IGN, LCA, ESA, GAU, etc.	SOL-1:1993.0–2009.0 SOL-2:1993.0–2015.0	Solution and Covariance matrix	Minimum constraints

the corresponding normal equations from Equation (2). Analogically, each weekly solution can produce one individual normal equation that can be stacked together later.

It is slightly different from Equation (2) when dealing with the VLBI input. Datum-free session-wise normal equations, other than solutions, are present in this case. This kind of normal equation is singular because a datum definition is lacking. There is no TRF transformation between the inputs and the combined solution, so $H_7^s(t_k)$ should be removed from Equation (2) in the VLBI case. In addition, the epoch of the EOP in VLBI input is different from that in the other three techniques. In order to combine the EOP of VLBI with the other three techniques, the epoch of the EOP has been transformed to the same epoch as other techniques except for UT1-UTC which is provided solely by VLBI.

All normal equations generated from all the weekly solutions or session-wise Normal EQuations (NEQs) can be stacked together to generate a normal equation system for each technique. Then we can add the normal equation system for each technique together to build a multi-technique normal equation system. It is worth mentioning that because there are large numbers of input files spanning so many years for each technique, the EOPs are especially computed as a daily average and the sets of TRF transformation parameters are produced for each weekly solution, hence the numbers of unknowns are also very large. In order to conserve memory in the computer and reduce the calculation time, an effective approach is to decompose the unknowns into global parameters and local parameters. The station coordinates at the reference epoch and the linear velocities can be regarded as global parameters. Also, the EOPs and the seven transformation parameters can be regarded as local parameters. Then the coefficient matrix in Equation (2) can be divided into two parts: $A1$ and $A2$. In detail, Equation (2) can be reduced to

$$\begin{pmatrix} X_i(t_i) \\ X_i^{\mathrm{eop}}(t_j) \end{pmatrix} = A1_i \begin{pmatrix} X_{\mathrm{c}}(t_0) \\ \dot{X}_{\mathrm{c}} \end{pmatrix} + A2_i \begin{pmatrix} H_7^s(t_k) \\ X_{\mathrm{c}}^{\mathrm{eop}}(t_j) \end{pmatrix}, \tag{3}$$

where i denotes the i-th weekly solution in all the weekly solutions. Then we can decompose the normal equation system into many sub-matrix blocks in the form of Equation (4).

$$\begin{pmatrix} \sum_{i=1}^{k} A1_i^T P_i A1_i & A1_1^T P_1 A2_1 & A1_2^T P_2 A2_2 & \cdots & A1_k^T P_k A2_k \\ A2_1^T P_1 A1_1 & A2_1^T P_1 A2_1 & 0 & \cdots & 0 \\ A2_2^T P_2 A1_2 & 0 & A2_2^T P_2 A2_2 & & 0 \\ \vdots & \vdots & & \ddots & \\ A2_k^T P_k A1_k & 0 & 0 & & A2_k^T P_k A2_k \end{pmatrix} \cdot \hat{x} = \begin{pmatrix} \sum_{i=1}^{k} A1_i^T P_i l_i \\ A2_1^T P_1 l_1 \\ A2_2^T P_2 l_2 \\ \vdots \\ A2_k^T P_k l_k \end{pmatrix} \tag{4}$$

where $P_1, \cdots, P_k$ are weighting matrices which can be obtained by the covariance matrix given in all the weekly solutions. Detailed information about the elements in $A1_1, \cdots, A1_k$ and $A2_1, \cdots, A2_k$ has been given in Altamimi et al. (2002).

Different types of constraints should be added to the NEQ system by using different methods, because the NEQ system derived only from the weekly solutions is not enough for the final combination. The constraints mainly contain: constraints about the datum definition of the combined terrestrial reference frame, constraints on local ties which link the different techniques together and velocity constraints connected to nearby stations or among the linear-wise solutions of one station which experiences abrupt changes or post-seismic motions.

From an observational point of view, space geodetic observations themselves do not carry any information about the datum definition of a refined coordinate system.

In the case of terrestrial reference frames, although space geodesy techniques are sensitive to some parameters related to the datum definition, for example, the dynamical techniques can 'see' the center of mass as the natural origin of the frame, they do not contain all the necessary information for the datum definition and all degrees of freedom of a frame are never simultaneously reduced to the same level in terms of physics (Sillard & Boucher 2001). From a practical point of view, a clearly and properly defined datum definition for the working coordinate system can be much more convenient for usage. From a mathematical point of view, the normal equation system constructed just upon space geodetic observations is certainly singular with a rank deficiency due to lack of information about the datum definition.

By following part of the IERS Conventions 2010 (Petit & Luzum 2010) about the definition of the ITRS and the datum of the ITRF, additional constraints about datum definition were added to the normal equation system generated from multiple techniques as follows: the origin of the combined reference frame is assumed to be the mean Earth center of mass and has zero translation rate with respect to the SLR time series, which is realized by SLR time series; similar to the origin, the scale of the frame has zero scale factor at epoch 2005.0 and zero scale rate with respect to weighted mean scale and scale rates of SLR and VLBI time series; the orientation is aligned to ITRF2008 by some core stations from four techniques by adding some constraints, i.e. the orientation parameters between ITRF2008 and our frame are zero at 2005.0 and the derivations are also zero. Two different types of constraints have been used: internal constraints to implement a linear frame and to preserve the intrinsic origin and scale in the SLR time series of weekly solutions and the scale in the VLBI time series of session-wise NEQs (Altamimi et al. 2007); and minimum constraints to remove uncertainties in the underlying combined terrestrial reference frame without any redundant conditions disturbing the natural construction of the TRF, see Sillard & Boucher (2001).

Local-ties at the co-location sites (Ray & Altamimi 2005) surveyed often by GPS or classical surveying are essential to the multi-technique combination of terrestrial reference frames. IERS has provided compiled local-tie information in SINEX format, which is the same as every single technique solution. These local-ties were introduced into the combination as extra "observations" by a coordinate-difference baseline model

$$\begin{cases} \Delta x_{\rm s} = x_{\rm s}^i - x_{\rm s}^j, \\ \Delta y_{\rm s} = y_{\rm s}^i - y_{\rm s}^j, \\ \Delta z_{\rm s} = z_{\rm s}^i - z_{\rm s}^j, \end{cases} \tag{5}$$

where $(x_{\rm s}^i, y_{\rm s}^i, z_{\rm s}^i)$ and $(x_{\rm s}^j, y_{\rm s}^j, z_{\rm s}^j)$ are the coordinates of points i and j respectively located at one co-location site. The covariance matrix of the baseline can be obtained by

$$\begin{aligned} D_{\Delta,s} &= K \cdot D_{ij,s} \cdot K^{\rm T}, \\ K &= \begin{pmatrix} 1 & 0 & 0 & -1 & 0 & 0 \\ 0 & 1 & 0 & 0 & -1 & 0 \\ 0 & 0 & 1 & 0 & 0 & -1 \end{pmatrix}, \end{aligned} \tag{6}$$

where $D_{ij,s}$ is the covariance matrix of co-location station coordinates and is also provided in the local-tie information files. The offset caused by applying such a baseline model to the datum definition is assumed to be negligible because of the short distance of the baseline.

3.2 Weighting

The weekly solutions of the station positions and the EOPs derived from different space geodetic techniques are computed by different technique-specific combination centers. Although each weekly solution is provided together with the full covariance matrix, the relative covariance levels between different techniques still need to be evaluated and we should implement an appropriate weighting scheme. Based on the assumption that the solutions from different techniques are statistically independent from each other, each technique-specific normal equation system was re-scaled by a multiplier factor, the so called covariance factor $^2_i(i = 1, 2, 3, 4)$. The determination of the covariance factors is a joint and iterative estimation process together with computation of the unknown parameters of the combined normal equation system.

The initial values are set to 1 for all $^2_i(i = 1, 2, 3, 4)$ at first, and then the combined normal equation system can be accumulated from the four individual normal equation systems according to

$$\begin{cases} N^{(1)} = \sum_{i=1}^4 \frac{1}{\sigma_i^{2\,(1)}} N_i^{(0)} + N_0^{(0)} \\ \qquad = \sum_{i=1}^4 1 \cdot N_i^{(0)} + N_0^{(0)} \\ w^{(1)} = \sum_{i=1}^4 \frac{1}{\sigma_i^{2\,(1)}} w_i^{(0)} + w_0^{(0)} \\ \qquad = \sum_{i=4}^4 1 \cdot w_i^{(0)} + w_0^{(0)} \end{cases} \tag{7}$$

Table 2 Covariance Factors of Four Techniques

Technique	SLR	GPS	VLBI	DORIS
Variance Factor	5.5	6.4	1.4	2.4

where $N_i^{(0)}$ and $w_i^{(0)}$ denote the sub-matrix and corresponding right-hand side decomposed to separate each technique input's contribution to the normal equation system respectively; $N_0^{(0)}$ and $w_0^{(0)}$ represent a partition of the normal equations, where no covariance factor will be estimated, such as the normal equations deduced from the datum constraints and velocity constraints. Then the unknown parameters are solved by

$$N^{(1)} \cdot \hat{x}^{(1)} = w^{(1)}. \tag{8}$$

Within each iteration step $k(k = 2, 3, \ldots)$, σ_i^2 can be computed by

$$\sigma_i^{2\,(k)} = \frac{v_i^T P_i v_i}{n_i - tr(N^{(k-1)^{-1}} N_i^{(k-1)})}, \tag{9}$$

where $v_i^T P_i v_i$ denotes the decomposed part from the contribution of the technique to the weighted sum of residuals; the denominator can be seen as the redundancy number of the respective technique.

After the updated $\sigma_i^{2\,(k+1)}$ has been obtained, the normal equation system can be updated according to

$$\begin{cases} N^{(k)} = \sum_{i=1}^{4} \frac{1}{\sigma_i^{2\,(k)}} N_i^{(k-1)} + N_0^{(k-1)} \\ w^{(k)} = \sum_{i=1}^{4} \frac{1}{\sigma_i^{2\,(k)}} w_i^{(k-1)} + w_0^{(k-1)}, \end{cases} \tag{10}$$

with

$$\begin{aligned} N_i^{(k-1)} &= \frac{1}{\sigma_i^{2\,(k-1)}} N_i^{(k-2)}, \\ w_i^{(k-1)} &= \frac{1}{\sigma_i^{2\,(k-1)}} w_i^{(k-1)} \end{aligned} \tag{11}$$

and

$$N_0^{(k-1)} = N_0^{(k-2)}, w_0^{(k-1)} = w_0^{(k-2)}. \tag{12}$$

The iterations are finished when convergence is reached.

Using the above method, the overall variance factor of the per-technique NEQs is estimated through an iteration process. Table 2 gives the values of the factors. It is worth noting that these factors are relative weights.

3.3 Discontinuities

For sites where there were episodic jumps, we applied the jumps given in the IGN SINEX files before 2009.0 and detected discontinuities caused by equipment changes or geophysical effects after 2009.0. Once we found a new discontinuity of one station, we divide that station's solution into two independent solutions before and after the discontinuity. When we analyze the residuals of all stations, we actually found some discontinuities, for example, as shown in Figure 3, GPS station AZCN(49504M001) had a jump in 2010. After we applied the piecewise model before and after that epoch, we combined once again, and then the station's residuals were much improved. The detection work was actually a combination of the 3-σ criterion and empirical judgment. Since 2009, we have found 50 discontinuities in GPS stations, three discontinuities in SLR stations and one discontinuity in VLBI stations.

4 RESULTS

4.1 Station Coordinates and Datum Definition

The most essential and critical part among the combined results is the 3-D coordinates of the stations using the four techniques that are distributed globally and the underlying network datum. The 7-parameter transformation model between two coordinate systems is the conventional method to assess the precision of the datum definition of the TRF. In the IERS Conventions 2010 (Petit & Luzum 2010), the transformation of a station's coordinates and the velocities in the TRS (1) to the TRS (2) are given by the equations below:

$$\begin{pmatrix} X_2 \\ Y_2 \\ Z_2 \end{pmatrix} = \begin{pmatrix} X_1 \\ Y_1 \\ Z_1 \end{pmatrix} + \begin{pmatrix} T_x \\ T_y \\ T_z \end{pmatrix} + \begin{pmatrix} D & -R_z & R_y \\ R_z & D & -R_x \\ -R_y & R_x & D \end{pmatrix} \begin{pmatrix} X_1 \\ Y_1 \\ Z_1 \end{pmatrix}, \tag{13}$$

$$\begin{pmatrix} \dot{X}_2 \\ \dot{Y}_2 \\ \dot{Z}_2 \end{pmatrix} = \begin{pmatrix} \dot{X}_1 \\ \dot{Y}_1 \\ \dot{Z}_1 \end{pmatrix} + \begin{pmatrix} \dot{T}_x \\ \dot{T}_y \\ \dot{T}_z \end{pmatrix} + \begin{pmatrix} \dot{D} & -\dot{R}_z & \dot{R}_y \\ \dot{R}_z & \dot{D} & -\dot{R}_x \\ -\dot{R}_y & \dot{R}_x & \dot{D} \end{pmatrix} \begin{pmatrix} \dot{X}_1 \\ \dot{Y}_1 \\ \dot{Z}_1 \end{pmatrix}, \tag{14}$$

where T_x, T_y and T_z are the three translation parameters along the x-, y- and z-axes; R_x, R_y and R_z are the rotation parameters along the corresponding axes. D is the scale parameter. The dot denotes linear time variation.

Table 3 lists the transformation parameters and their rates from SOL-1 to ITRF2008 and DTRF2008, from SOL-2 to ITRF2008 and ITRF2014 as well as from SOL-1 to SOL-2. Regarding the translation parameters, T_x and T_y from SOL-1 to ITRF2008 or DTRF2008 are both smaller than 0.1 mm with rates better than 0.3 mm yr^{-1}. But T_z between SOL-1 and ITRF2008 is 3.4 mm, which is significantly larger than T_z from SOL-

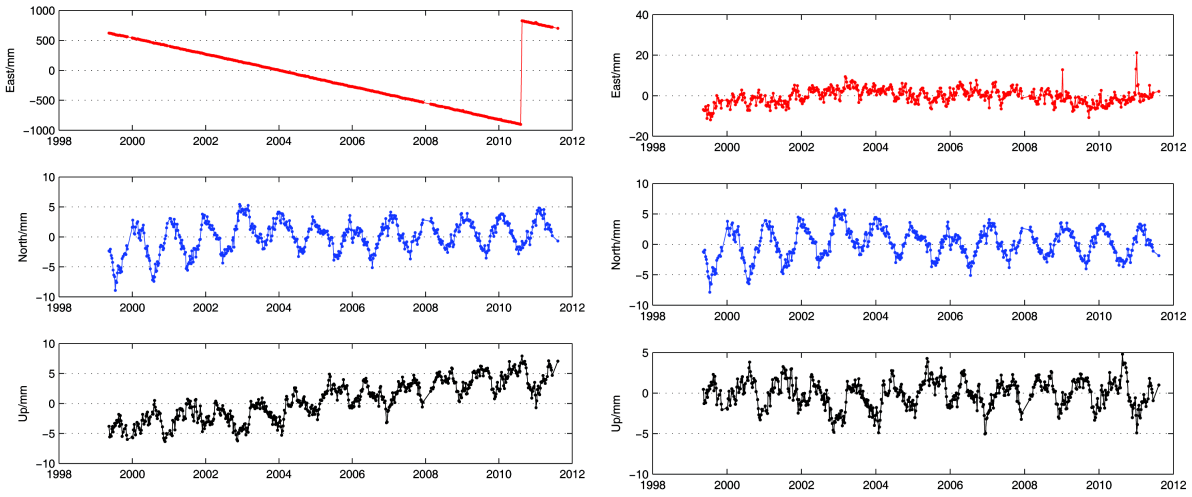

Fig. 3 Residuals of station 49504M001 before (*right*) and after (*left*) applying discontinuity.

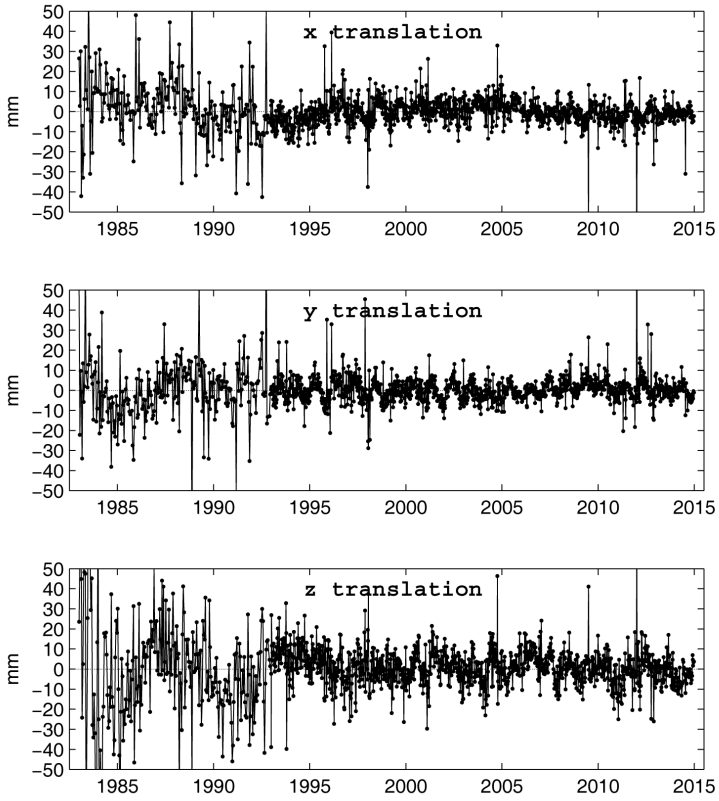

Fig. 4 Time series of translation parameters from weekly solutions of SLR station coordinates to the long-term combined solution SOL-2 based on SLR, GPS, VLBI and DORIS.

1 to DTRF2008 (–1.0 mm). T_x, T_y and T_z from SOL-2 (solution 2) to ITRF2008 are 1.5, 0.7 and 4.0 mm with rates smaller than 0.6 mm yr^{-1}. Large T_z also happened between SOL-2 and ITRF2008 similar to SOL-1. T_x, T_y and T_z from SOL-2 to ITRF2014 are 2.2, -1.8 and -0.9 mm respectively with rates smaller than 0.4 mm yr^{-1}. SOL-1 and SOL-2 are calculated by the same combination strategy and the same procedure but based on different cut-off epochs of input, and the translation parameters are –1.4, –0.7 and –0.7 mm, respec-

Table 3 Comparison of Transformation Parameters at Epoch 2005.0 and Their Rates From SOL-1 to ITRF2008, SOL-1 to DTRF2008, SOL-2 to ITRF2008, SOL-1 to SOL-2, as well as Parameters at Epoch 2010.0 and Their Rates From SOL-2 to ITRF2014

	T_x (mm)	T_y (mm)	T_z (mm)	D (ppb)	R_x (mas)	R_y (mas)	R_z (mas)
	$\dot{T}_x$ (mm yr^{-1})	$\dot{T}_y$ (mm yr^{-1})	$\dot{T}_z$ (mm yr^{-1})	$\dot{D}$ (ppb yr^{-1})	$\dot{R}_x$ (mas yr^{-1})	$\dot{R}_y$ (mas yr^{-1})	$\dot{R}_z$ (mas yr^{-1})
SOL-1 to ITRF2008	0.0 (±0.1)	0.0(±0.1)	3.4(±0.1)	–0.77(±0.02)	0.03(±0.00)	–0.01(±0.00)	0.01(±0.00)
	–0.2(±0.1)	–0.2(±0.1)	–0.2(±0.1)	0.02(±0.02)	0.00(±0.00)	0.00(±0.00)	0.00(±0.00)
SOL-1 to DTRF2008	0.0(±0.3)	0.1(±0.4)	–1.0(±0.4)	–0.19(±0.06)	0.01(±0.01)	–0.03(±0.01)	0.03(±0.01)
	0.2(±0.3)	–0.1(±0.4)	–0.1(±0.4)	–0.07(±0.06)	0.00(±0.01)	0.00(±0.01)	0.00(±0.01)
SOL-2 to ITRF2008	1.5(±0.2)	0.7(±0.2)	4.0(±0.2)	–0.55(±0.03)	0.03(±0.01)	–0.02(±0.01)	0.04(±0.01)
	0.1(±0.2)	–0.2(±0.2)	–0.5(±0.2)	0.05(±0.03)	0.00(±0.01)	0.00(±0.01)	0.00(±0.01)
SOL-2 to ITRF2014	2.2(±0.7)	–1.8(±0.8)	–0.9(±0.7)	–0.31(±0.13)	0.02(±0.03)	–0.10(±0.03)	0.09(±0.03)
	0.3(±0.7)	–0.1(±0.8)	–0.3(±0.7)	0.00(±0.13)	–0.01(±0.03)	0.01(±0.03)	0.01(±0.03)
SOL-1 to SOL-2	–1.4(±0.1)	–0.7(±0.1)	–0.7(±0.1)	–0.16(±0.01)	–0.01(±0.00)	0.01(±0.00)	–0.03(±0.00)
	–0.3(±0.1)	0.0(±0.1)	0.2(±0.1)	–0.04(±0.01)	0.00(±0.00)	0.00(±0.00)	–0.01(±0.00)

Table 4 Annual amplitude and phase fitted to the time series of translation parameters from SLR weekly solutions to long-term combined solutions SOL-1 and SOL-2.

		T_x	T_y	T_z
SLR w.r.t. SOL-1	A (mm)	2.2±0.2	3.3±0.2	3.5±0.3
	ϕ (°)	44±5	316±3	8±5
SLR w.r.t. SOL-2	A (mm)	2.2±0.2	3.1±0.1	3.4±0.3
	ϕ (°)	53±4	315±2	11±5

tively. The scale parameter from SOL-1 to DTRF2008 is also smaller than that from SOL-1 to ITRF2008. They are -0.19 ppb and -0.77 ppb, respectively. Their rates are both smaller than 0.1 ppb yr^{-1}. The scale parameter and the rate from SOL-1 to SOL-2 are -0.16 ppb and -0.04 ppb yr^{-1} respectively. The rotation parameters in Table 3 are all smaller than 0.05 mas and their rates are smaller than 0.02 mas yr^{-1}, except for the case of SOL-2 to ITRF2014.

Underlying linear TRFs have been realized in the combined solutions SOL-1 and SOL-2 with the origin defined solely by SLR input data while the scale is defined by both SLR and VLBI input data. Considering that the input time span of SOL-2 covers that of SOL-1 and then extends to 2015.0, Figure 4 illustrates the time series of translation parameters of the SLR input with respect to SOL-2 over the whole input time span. We did not see a small offset in the Y component around 2010, which has been published in Altamimi et al. (2016). Since the observation data of Lageos-2 was applied in 1993, the scatter of the temporal variations of the translation parameters has been much smaller than before and the accuracy of the origin can be better than 1 cm but cannot reach the sub-mm level. The annual signal of the time series in Figure 4 as well as that of the SOL-1 case are fitted by a cosine function and the amplitudes and phases are displayed in Table 4. Compared with similar results of ITRF2008 (Altamimi et al. 2011) and ITRF2014 (Altamimi et al. 2016), differences between either the amplitude or the phase of the x or y component of our combined solutions and ITRF are small (amplitude differences smaller than 0.5 mm and phase differences smaller than 8°) but the difference in the z component is large. The contrasting results of z translation are also listed in Table 3.

The scale of the combined solutions was defined by the weighted mean of SLR and VLBI input data. Figure 5 displays the scale factors of SLR and VLBI with respect to SOL-2. Similarly as the SLR translation parameters shown in Figure 4, Lageos1-only observations before 1993.0 make the SLR scale factors have larger scatter than after it. Small drifts could be seen both in the early years and the latest years of the VLBI time series.

Figures 6 and 7 show the SOL-2 horizontal and vertical velocities for the sites with formal error less than 0.3 mm yr^{-1}. The geophysical interpretation of velocity fields and a detailed comparison among velocities of the local ties are included in future investigation plans.

After transforming the station coordinates in SOL-1 to the values in ITRF2008 by using the corresponding

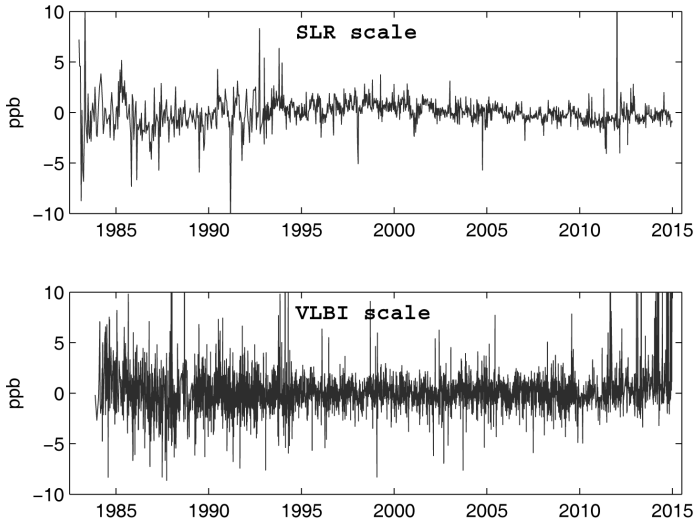

Fig. 5 Time series of scale factors transforming from SLR weekly (*upper*) or VLBI session-wise (*lower*) solutions to the long-term combined solution SOL-2 of four techniques: SLR, VLBI, GPS and DORIS.

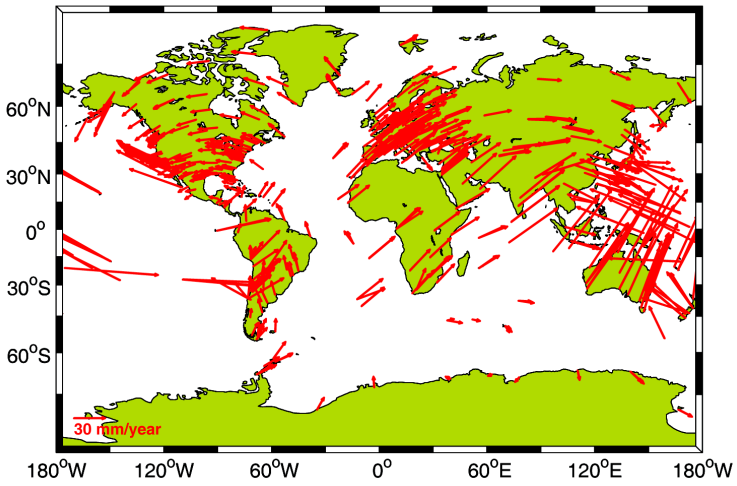

Fig. 6 Horizontal site velocities with formal error less than 0.3 mm yr^{-1}.

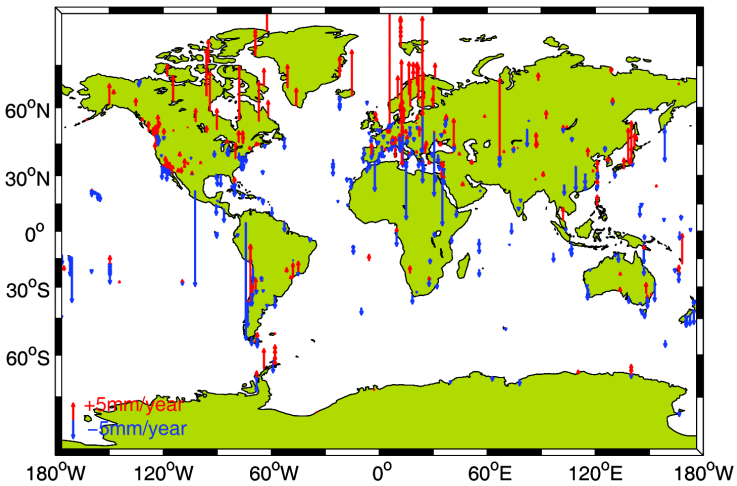

Fig. 7 Vertical site velocities with formal error less than 0.3 mm yr^{-1}.

7-parameter transformations, we then calculate the total root mean square (RMS) of the residual differences in three dimensions for each site-coordinate solution (two solutions are considered before and after the discontinuities happened) between SOL-1 and ITRF2008.

Figure 8 displays the 3-D RMS (y axis) of the coordinates' residuals between SOL-1 and ITRF2008 by removing the 7-parameter transformation effect with respect to (w.r.t.) the average numbers (x axis) of weekly solutions per year calculated from the numbers of input SINEX files divided by length of years of the observations for each site (we call it average "observation" numbers hereafter). More than one set of XYZ coordinates has been provided for those stations where discontinuities have happened. Although the relationship between the average "observation" numbers and the coordinate RMS of SLR stations is not totally positive, relatively low RMS can be commonly seen when average "observation" numbers per year are greater than 20. Expectations are present perhaps for stations with discontinuities and consequently velocities before and after the discontinuities happened, which are constrained to be equal among different solutions. A similar phenomenon can be seen in VLBI. Therefore, the velocity constraints on stations with discontinuities should be carefully applied. The average "observation" numbers for GPS station coordinate solutions are concentrated within the interval of 30–50 per year. The observational activity of GPS stations is more stable than that of VLBI or SLR. However, a large amount of GPS stations has more than one discontinuity that happened and several solutions are calculated for each of the stations. When the time span of one of the solutions is clearly short and velocities of all of the solutions are constrained to be equal, the RMS of each solution for this kind of station will be influenced. The "observation" numbers of DORIS stations are also stable and concentrated but the RMS level is generally higher than the other three techniques.

4.2 The Combined EOPs

The other important combination is the combination of EOPs from the four techniques. Daily polar motions are provided by the mean of the day from GPS, SLR and DORIS. The polar motions from VLBI input were propagated to the same epoch through the corresponding rates during the combination process. Only the LODs from GPS and VLBI were considered during the combination.

For external calibration, differences between IERS EOP 08 C04 and the combined EOPs of SOL-1 or SOL-2 are calculated and displayed in Figure 9. Firstly, no significant bias or drift can be seen in the combined EOP results w.r.t. IERS EOP 08 C04. The agreement was quite good for the two solutions SOL-1 and SOL-2 overall. For the x-component and y-component of the polar motion, both the SOL-1 and SOL-2 time series showed significantly smaller noise for the time when GPS contributes. A similar result could be observed for LOD.

The WRMS and RMS of the time series of EOP difference by the SOL-1 minus IERS EOP 08 C04 and by the SOL-2 minus IERS EOP 08 C04 are given in Table 5. The WRMS values of the polar motions, UT1-UTC and the LODs from SOL-1 or SOL-2 are all smaller than those derived from DTRF2008 minus IERS EOP 08 C04 published in Seitz et al. (2012).

5 CONCLUSIONS

A combination method based on years of weekly solutions from SLR/GPS/DORIS and session-wise normal equations from VLBI was developed at SHAO to generate a long-term and global TRF and consistent EOP series. In order to compare with the ITRF2008 and ITRF2014, two solutions, namely SOL-1 and SOL-2, were estimated based on different time spans of input data. The input of SOL-1 ends with 2009.0, the same as that of ITRF2008. The input of SOL-2 ends with 2015.0. Each combined solution includes 3-D coordinates of the space geodetic stations distributed globally and consistent daily EOP values at the epoch given by the weekly input solutions.

Compared with ITRF2008 and DTRF2008, the precision of the x-component and y-component of SOL-1's origin was better than 0.1 mm and their rates are better than 0.3 mm yr^{-1}. The transformation parameter T_z from SOL-1 to ITRF2008 and DTRF2008 were 3.4 mm and -1.0 mm, respectively. It means that the z-component of the SOL-1 origin was much closer to DTRF2008 than ITRF2008. Compared to SOL-1, five more years of input data from four techniques significantly impacted the SOL-2 origin by the level of 1.4 mm in the x-component and 0.7 mm in the y-component. The translation parameters from SOL-2 to ITRF2014 were 2.2, -1.8 and 0.9 mm in x-, y- and z-components respectively with their rates smaller than 0.4 mm yr^{-1}. Similar to the origin, the scale of SOL-1 was much closer to that of DTRF2008 than ITRF2008. The scale parameter from

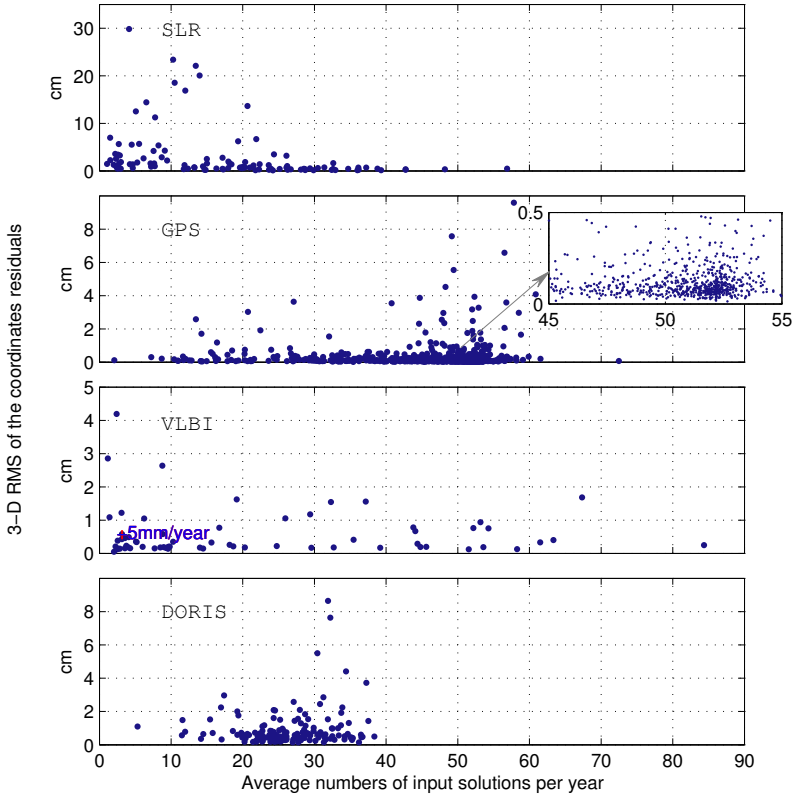

Fig. 8 The 3-D RMS of the coordinate residuals of SOL-1 w.r.t. ITRF2008 corresponding to the average numbers of weekly or session-wise solutions per year of each station.

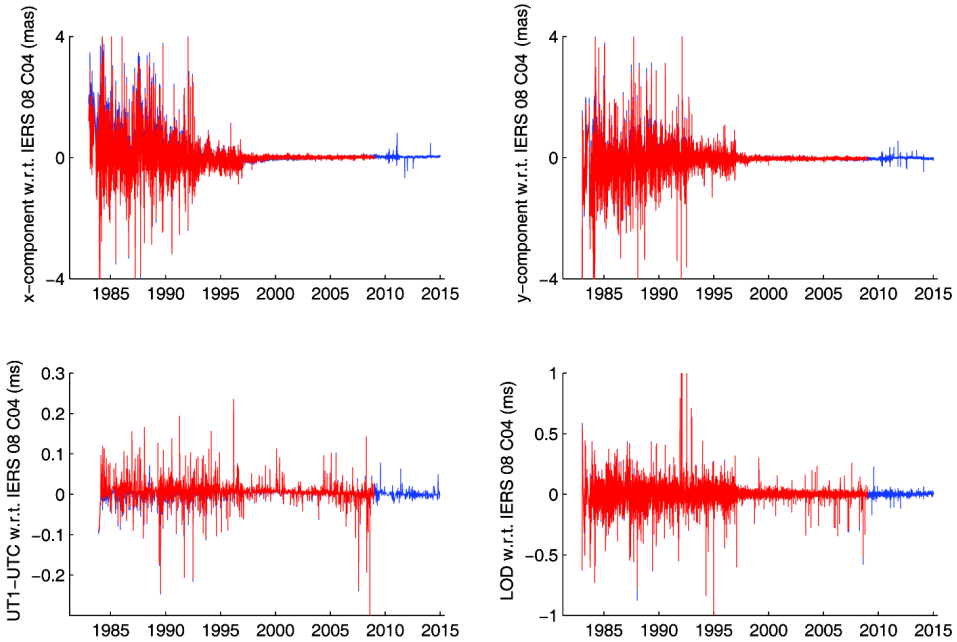

Fig. 9 Comparison of the polar motions, the UT1-UTC and the LODs of the combined solutions SOL-1 and SOL-2 w.r.t. IERS EOP 08 C04.

Table 5 WRMS and RMS Values of the EOP Differences From Combined Solutions SOL-1/SOL-2 Minus IERS EOP 08 C04

Parameter	WRMS		RMS	
	SOL-1	SOL-2	SOL-1	SOL-2
x-component of polar motion (mas)	0.048	0.045	0.469	0.422
y-component of polar motion (mas)	0.057	0.048	0.444	0.392
UT1-UTC (ms)	0.009	0.008	0.027	0.025
LOD (ms)	0.017	0.011	0.078	0.069

SOL-2 to ITRF2014 was -0.31 ppb with its rate lower than 0.01 ppb.

In the time series of translation parameters from weekly SLR solutions to SOL-2, we did not see a small offset in the y-component around 2010 which has been published in Altamimi et al. (2016). By fitting to a cosine function, differences between either the amplitude or phase of the x and y components of our combined solutions and the ITRF were small (the amplitude differences were smaller than 0.5 mm and the phase differences were smaller than 8°) but the difference of the z component was large.

By analysis of the 3-D RMS of each station's positions with respect to ITRF2008, averaged numbers of observations per year have an obvious effect on the accuracy of SLR stations. However, SLR is the only technique that contributes to the origin of the combined terrestrial reference frame, which calls for upgrading the observing ability of SLR stations to increase the precision of the origin of the combined TRF.

Compared with IERS EOP 08 C04, WRMS of the consistently combined EOP series was smaller than 0.06 mas for the polar motions, smaller than 0.01 ms for the UT1-UTC and smaller than 0.02 for the LODs. The precision of the EOPs in SOL-2 is slightly higher than that of SOL-1.

Acknowledgements We thank ILRS, IGS, IVS and IDS for providing the short-term solutions of station positions and Earth Orientation Parameters in SINEX format. We also thank IERS(IGN/DGFI) for providing their study of TRF and EOP for comparison with our results. This work was supported by the Ministry of Science and Technology of China (2015FY310200), the National Key Research and Development Program of China (2016YFB0501405), the National Natural Science Foundation of China (11173048 and 11403076), the State Key Laboratory of Aerospace Dynamics and the Crustal Movement Observation Network of China (CMONOC).

References

Altamimi, Z., Collilieux, X., Legrand, J., Garayt, B., & Boucher, C. 2007, Journal of Geophysical Research: Solid Earth, 112, 83

Altamimi, Z., Collilieux, X., & Métivier, L. 2011, Journal of Geodesy, 85, 457

Altamimi, Z., Rebischung, P., Métivier, L., & Collilieux, X. 2016, Journal of Geophysical Research (Solid Earth), 121, 6109

Altamimi, Z., Sillard, P., & Boucher, C. 2002, Journal of Geophysical Research: Solid Earth, 107, ETG 2-1

Angermann, D., Drewes, H., Gerstl, M., Krügel, M., & Meisel, B. 2009, in Geodetic Reference Frames (Springer), 134, 11

Blewitt, G. 2003, Journal of Geophysical Research: Solid Earth, 108

Blewitt, G., Altamimi, Z., Davis, J., et al. 2010, in Understanding Sea-level Rise and Variability, eds., J. A. Church, et al. (Oxford: Wiley-Blackwell), 256

Bloßfeld, M., Seitz, M., & Angermann, D. 2014, Journal of Geodesy, 88, 45

Bloßfeld, M., Roggenbuck, O., Seitz, M., Angermann, D., & Thaller, D. 2015, in EGU General Assembly Conference Abstracts, 17, 2013

Böckmann, S., Artz, T., & Nothnagel, A. 2010, Journal of Geodesy, 84, 201

Dow, J. M., Neilan, R. E., & Rizos, C. 2009, Journal of Geodesy, 83, 191

Ferland, R., & Piraszewski, M. 2009, Journal of Geodesy, 83, 385

Heflin, M., Jacobs, C., Sovers, O., Moore, A., & Owen, S. 2013, in Reference Frames for Applications in Geosciences (Springer), 267

Jin, S., Zhang, L. J., & Tapley, B. D. 2011, Geophysical Journal International, 184, 651

Jin, S., van Dam, T., & Wdowinski, S. 2013, Journal of Geodynamics, 72, 1

Koch, K.-R. 2013, Parameter Estimation and Hypothesis Testing in Linear Models (Springer Science & Business Media)

Kutterer, H., Seitz, F., Alkhatib, H., Schmidt, M., et al. 2015, in The 1st International Workshop on the Quality of Geodetic

Observation and Monitoring Systems (QuGOMS'11), International Association of Geodesy Symposia 140, eds., H., Kutterer, F. Seitz, H. Alkhatib, M. Schmidt (Springer), 57

Pavlis, E. C., Luceri, C., Sciarretta, C., & Evans, K. 2014, in EGU General Assembly Conference Abstracts, 16, 4079

Pearlman, M. R., Degnan, J. J., & Bosworth, J. 2002, Advances in Space Research, 30, 135

Petit, G., & Luzum, B. 2010, IERS Technical Note, 36, 1

Ray, J., & Altamimi, Z. 2005, Journal of Geodesy, 79, 189

Schuh, H., & Behrend, D. 2012, Journal of Geodynamics, 61, 68

Seitz, M., Angermann, D., Bloßfeld, M., Drewes, H., & Gerstl, M. 2012, Journal of Geodesy, 86, 1097

Seitz, M., Angermann, D., & Drewes, H. 2013, in Reference Frames for Applications in Geosciences (Springer), 138, 87

Sillard, P., & Boucher, C. 2001, Journal of Geodesy, 75, 63

Thaller, D., et al. 2008, Inter-technique Combination based on Homogeneous Normal Equation Systems Including Station Coordinates, Earth Orientation and Troposphere Parameters, Scientific Technical Report STR08/15, Deutsches GeoForschungsZentrum Potsdam, Germany

Valette, J.-J., Lemoine, F. G., Ferrage, P., et al. 2010, Advances in Space Research, 46, 1614

Willis, P., Fagard, H., Ferrage, P., et al. 2010, Advances in Space Research, 45, 1408

Wu, X., Abbondanza, C., Altamimi, Z., et al. 2015, Journal of Geophysical Research (Solid Earth), 120, 3775